Application of click-click chemistry to the synthesis of new multivalent RGD conjugates.

Mathieu Galibert, Lucie Sancey, Olivier Renaudet, Jean-Luc Coll, Pascal Dumy, Didier Boturyn

ARTICLE TYPE www.rsc.org/xxxxxx | XXXXXXXX

Application of click-click chemistry to the synthesis of new multivalent RGD conjugates

Mathieu Galibert,[a] Lucie Sancey,[b] Olivier Renaudet,[a] Jean-Luc Coll,[b] Pascal Dumy[a] and Didier Boturyn[a]*

Received (in XXX, XXX) Xth XXXXXXXXX 200X, Accepted Xth XXXXXXXXX 200X
First published on the web Xth XXXXXXXXX 200X
DOI: 10.1039/b000000x

New multivalent RGD-containing macromolecules were designed

Introduction

The design and the synthesis of targeting molecules for diagnostic and therapeutic applications represent a major goal in cancer medicine. To this end, peptide ligands for various targets have been identified using combinatorial libraries [1] or phage display method.[2] To attain improved activity and receptor selectivity, it is often essential to restrict the conformational space of peptides by using them in a cyclic form.[3] In this context, cyclic peptides encompassing RGD (Arg-Gly-Asp) sequence have served as the basis for the development of potent peptide ligands used to selectively target the $\alpha_V\beta_3$ integrin.[4] The latter represents an attractive target for cancer therapeutic purposes.[5] Furthermore, it is well known that the multivalent display of a ligand enhances the binding strength of the ligand to its receptor and can promote receptor-mediated internalisation of the bound entity.[6] Today, the principle of multivalency has then been recognized as an important strategy for the design of synthetic ligands.[7] The effect of multivalency in ligand binding was particularly demonstrated for glycoconjugates,[8] and for peptide ligands.[9] Enhancements of biological activity were especially obtained from multivalent RGD (Arg-Gly-Asp) peptide ligand used to target cell surface receptors such as $\alpha_V\beta_3$ integrin.[10]

Recently, we have shown that tetrameric RGD-containing scaffolds exhibit desirable biological properties for tumour imaging [11] and for targeted drug delivery.[12] These compounds contain a cluster of four copies of a cyclo[-RGDfK-] monomer grafted onto a cyclic decapeptide scaffold (Fig. 1). Pioneering work aimed at studying the effect of the multivalency parameter in terms of interaction between the ligand and the target receptor and examining the contribution of each c[-RGDfK-] motif. For this purpose, we designed an array of peptide derivatives containing from one to four copies of the c[-RGDfK-] monomer (Fig. 1).[13] In order to obtain ligands with similar shape, similar steric hindrance and close molecular weights, which is essential for their comparison *in vitro*, we opted to substitute c[-RGDfK-] for non sense c[- RβADfK-] motifs in the ligands whose valency was lower than four. We used a combinatory assembling strategy to explore all possible positions of the RGD motifs on the cyclodecapeptide scaffold. Consequently, we were unable to isolate the different isomers that differ in the position of cyclic RGD pentapeptides onto the cyclodecapeptide scaffold. To overcome this problem, we recently reported an orthogonal chemoselective ligation strategy that allow access to well defined biomolecular assemblies by exploiting the Huisgen dipolar cycloaddition and the oxime bond formation.[14] Following this strategy, herein we describe the synthesis of new multivalent RGD compounds such as the fluorescent carbohydrate conjugate **1** (Scheme 1). The incorporation of the carbohydrate moiety may provide an enhanced solubility and clearance. With the molecules in hand, we then concentrated our work on assessing biological activities to determine the potency of the different RGD-containing compounds.

Fig. 1 Structure of clustered RGD-containing compounds.

Results and discussion

Chemical assemblies

Scheme 1 illustrates the approach used for the synthesis of compounds **1**-**2**. The biomolecular assembling process implies two chemoselective ligations (click-click chemistry): the oxime ligation [15] and the Cu(I)-catalyzed azide-alkyne cycloaddition (CuAAC).[16] To introduce suitable functions within peptide moities, we synthesized building blocks such as compounds **3** and **4** which contain protected serine (masked aldehyde) and alkyne groups, respectively (Scheme 1). The use of building blocks during the solid-phase peptide synthesis (SPPS) reduces the number of steps involved for the construction of such conjugates.[17]

Scheme 1 Synthesis of compounds **1**-**2**. a) Standard Fmoc/t-Bu Solid-Phase Peptide Synthesis; b) PyBOP (1 equiv.), DIPEA (4 equiv.), 1 h; c) TFA/H_2O (95:5), 2 h; d) $NaIO_4$ (10 equiv.), 30 min; e) **8** (6 equiv.), **9** (3 equiv.), *t*-BuOH/H_2O/AcOH (50:45:5), Cu(0) microsize powder (0.5 mg), 2 h then pH 7.0, 18 h; For X = Lys, then Cy5-OSu (1 equiv.), DMF, DIPEA (pH 8), 3 h.

In this context, linear peptides encompassing chemoselective ligations were prepared following rigorously the standard Fmoc/*t*-Bu SPPS procedure using PyBOP as coupling reagent. The head-to-tail cyclizations provided the desired cyclodecapeptide scaffolds **5** and **6**. Deprotection of serine residue using a concentrated TFA solution followed by a subsequent oxidation with periodate [18] afforded key intermediates **7** and **8**, isolated in sufficient purity to carry out subsequent chemoselective assemblies. In parallel, RGD-containing cyclopentapeptide **9** bearing the prerequisite azide function and aminooxy-carbohydrate **10** were prepared as described.[14,8g] Very recently, we have shown that cyclopeptide assemblies are possible by means of orthogonal oxime and copper-mediated click reactions in a stepwise or in a one-pot approach.[14] The latter method is much desired, as it avoids lengthy separation process and purification of intermediates while increasing overall chemical yield. Biomolecular ligations of azidopeptide **9** and aminooxy-carbohydrate **10** were then performed on either molecular scaffold **7** or **8**. Peptides **7**, **9** (6 equiv.) and carbohydrate **10** (3 equiv.) were applied under mild acidic conditions using a solution containing dilute acetic acid and copper microsize powder. Rapid oxime ligation of **10** was observed (Figure 2). Neutralizing the pH resulted in complete disappearance of the intermediate and the exclusive formation of the expected compound **2**.

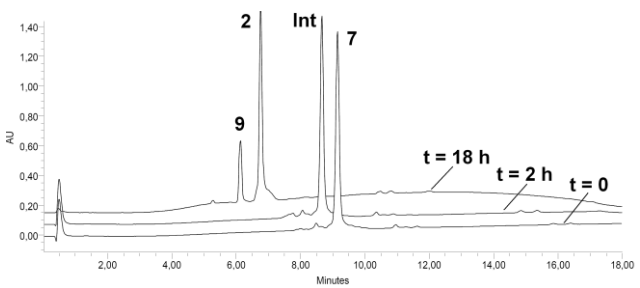

Fig. 2 One-pot chemoselective assembly of peptides **7**, **9**, and carbohydrate **10**. HPLC traces are shown at 2 h and 18 h. Int=intermediate.

Fig. 3 Structure of compounds **12**-**18**.

To evaluate the RGD-containing compounds for further *in vivo* studies, we decided to introduce a fluorescent reporter such as Cyanine 5 (Cy5) because its near-infra red (NIR) band (λ_{em} = 670 nm) can penetrate tissue up to 6 cm allowing non invasive optical imaging in small animals. Furthermore, this NIR band is absent of interfering biofluorescence. For this purpose, the intermediate **11** was synthesized according the procedure described above. Cy5 dye was then introduced at the lysine side-chain of **11** under neutral conditions (pH 8.0) affording the fluorescent conjugate **1** in 72% yield after RP-HPLC purification. Compounds **1** and **2** were characterized by ES-MS and the observed molecular weights were found in excellent agreement with the calculated values.

To study the contribution of each c[-RGDfK-] motif, an array of molecules **12-19** was designed and prepared according to the method previously described (Figure 3).[12a,14] Briefly, RGD ligands and nonsense RβAD peptides were introduced onto the scaffold by using respectively the Huisgen dipolar cycloaddition and orthogonal oxime bond formation, the latter providing shorter linker.

Biological assays

The adhesion potency of the different multivalent RGD-containing peptides was first determined using a traditional ELISA-type inhibition assay. In this experiment, we measured the efficiency of peptides to compete with vitronectin, the natural substrate of the $\alpha_V\beta_3$ integrin, when binding to HEK-β3 cells that overexpress $\alpha_V\beta_3$ receptors. HEK-β3 cells were therefore incubated with soluble compounds **2**, **12-18** at 37 ◦C onto vitronectin-coated assay plates. The IC50 values, or concentration of compounds required to inhibit 50% of the cells from attaching to vitronectin, are reported in Table 1. As expected the negative control peptide **13** did not inhibit cell adhesion to vitronectin as reported for compound analogues.[10d,13] Increasing the number of RGD motifs from 1 to 3 gradually improved the potency of the ligand to compete with vitronectin. We reasoned that the observed multivalent effect arises from a statistical rebinding of the RGD-containing compound due to the high local concentration of RGD moieties. This phenomenon was observed for dendrimer scaffold.[8f] It is worth noting that compounds **16** and **17** that differ in the position of the RGD units onto the cyclodecapeptide scaffold show similar IC50 (respectively, 7.1 and 8.2 µM). The position of the RGD peptides onto the cyclodecapeptide scaffold does not improve the affinity of the molecule. Compounds that display four RGD units (i.e. molecules **2**, **12** and **13**) showed potent inhibitory effect. Nevertheless, IC50 values for compounds **2** and **14** (respectively, 3.8 and 4.1 µM) are slightly lower than the value obtained for compound **12** (4.9 µM) encompassing shorter oxime linkers. Surprisingly, the molecule **15** encompassing three RGD units displayed the best IC50 (2.8 µM). We previously showed that compounds including three or four RGD ligands exhibit close IC50.[13] We argue that the shorter oxime linker used to graft non-sense RβAD peptide within molecule **15** generates less steric hindrance than unbinded RGD moieties within molecules **2**, **12** or **13** while the RGD-containing compound binds to $\alpha_V\beta_3$ receptor.

Table 1 Competitive cell adhesion assay

Compounds			
#	RGD unit/ molecule	IC50 (µM) [a]	Standard deviation (µM) [a]
12	4	4.85	0.19
13	0	NI [b]	-
14	4	4.10	0.08
15	3	2.80	0.15
16	2	7.13	0.36
17	2	8.22	0.16
18	1	48.81	0.24
2	4	3.77	0.11

[a] Values were determined from three separate experiments; [b] NI, no inhibition was observed.

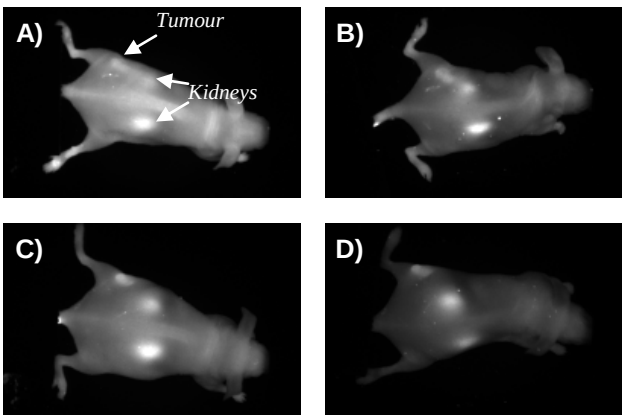

Fig. 4 Representative images of optical imaging of subcutaneous tumour-bearing mice observed at (A-C) 1 h and (B-D) 3 h after iv injection of (A-B) 10 nmol **19** and (C-D) 10 nmol **1**.

We then measured the capacity of the molecules to target tumour in mouse. Figure 4 shows typical FRI images of nude mice bearing an subcutaneous human TS/A-pc tumour at different time points after intravenous (iv) injection of 10 nmol fluorescent molecules (i.e. **1** or **19**) (See also the Supplementary Information). Strong signal is observed in the kidneys reflecting the prominent and fast renal excretion of RGD-containing molecules as previously shown.[11] One hour postinjection, fluorescent molecules accumulate in the tumour but the whole body is also fluorescent due to the presence of unbound circulating molecules. The average values for the tumour/skin ratios were found to be similar for mice treated with **1** and for mice treated with **19** (respectively 1.39 ± 0.37 and 1.32 ± 0.15) (See Table S1 in the Supplementary Information). The contrast (tumour/skin ratio) was found to be statistically better with **1** (Figure 4D) 3 h after iv injection while the ratio was lower at late time. In comparison, tumour/skin ratio for mice treated with **19** reaches its maximum at 6 h, and then slowly decreases (See the Supplementary Information). These experimental results are in good agreement with a better clearance of the carbohydrate-containing compound **1**.

Conclusions

We have expanded the scope of click–click chemistry by gaining access to new RGD-containing macromolecules. For instance, we have shown that biomolecular assembly combining carbohydrate and peptides is possible by means of orthogonal oxime and copper-mediated click reactions in a one-pot synthesis. This approach is part of the general trend of organic chemistry taking control of macromolecule synthesis to produce well-defined constructs that could likely become the rule in drug applications. The ensuing RGD compounds were then evaluated through competitive cell adhesion assays and *in vivo* experiments. The results obtained highlight the utility of a clustered ligand, and as expected the grafting of an additional carbohydrate enhances clearance of the RGD-containing compound. It is worth noting that our approach is not limited to integrin ligands, it may be conceptually exploited to synthesize other sophisticated macromolecular conjugates.

Experimental

Cyclodecapeptide scaffolds 5. Linear decapeptides were assembled on 2-chlorotritylchloride® resin (150 mg, loading of 0.8 mmol/g) using the general procedure (See the Supplementary Information) by using building blocks **3** and **4.** The cyclization reaction were carried out in DMF using linear peptide (172 mg, 100 µmol, 0.5 mM) and PyBOP (1 equiv.) for 1 h at room temperature. After completion of the reaction, the solvent was evaporated and the cyclic peptide **5** was obtained as a white solid powder after ether precipitation (161 mg, 100 µmol, quantitative yield). Mass spectrum (ES-MS, positive mode) calc for $C_{79}H_{122}N_{16}O_{18}$: 1583.95, found m/z: 1584.0.

Cyclodecapeptide scaffolds 6. Following the procedure previously described and starting with linear peptide (171 mg, 92 µmol), cyclic peptide **5** was obtained as a white solid powder (167 mg, 96 µmol, 96 % yield). Mass spectrum (ES-MS, positive mode) calc for $C_{87}H_{137}N_{17}O_{20}$ 1741.16, found m/z : 1740.9.

Cyclodecapeptide scaffolds 7. Full deprotection of peptide **5** (161 mg, 100 µmol) was carried out in a solution containing 10 mL of TFA/H_2O (95:5) for 2 h at room temperature. The product was isolated after removal of solvents under reduced pressure and precipitation from Et_2O. A serine oxidation by an aqueous solution containing $NaIO_4$ (10 equiv.) afforded the peptide **7**. The crude product was directly purified by using RP-HPLC affording the compound **7** as a white powder. (72 mg, 48 µmol, 48 % yield). Mass spectrum (ES-MS, positive mode) calc for $C_{69}H_{101}N_{15}O_{16}$: 1396.67, found m/z : 1396.7.

Cyclodecapeptide scaffolds 8. Following the procedure previously described and starting with cyclic peptide **6** (167 mg, 96 µmol), peptide **8** was obtained as a white powder. (60 mg, 41 µmol, 43 % yield). Mass spectrum (ES-MS, positive mode) calc for $C_{72}H_{108}N_{16}O_{16}$ 1453.76, found m/z : 1453.8.

Peptide 2. To a solution containing the cyclodecapeptide **7** (5 mg, 3.5 µmol) in 500 µL of *t*BuOH/H_2O/AcOH (50:45:5) were added the compound **9** *c*[-RGDfK($COCH_2N_3$)-] (6 equiv.) , the compound **10** Glc-β-ONH_2 (3 equiv.) and Cu(0) microsize powder (5 equiv.). The reaction mixture was stirred for 2 h at room temperature. Then, the pH was adjusted to 8 by addition of a $NaHCO_3$ solution (10 %). The reaction mixture was stirred overnight at room temperature. The reaction mixture was centrifuged for 5 min and the solution was purified by RP-HPLC to give the desired compound **2** (5.2 mg, 1.2 µmol, yield 34 %). Mass spectrum (ES-MS, positive mode) calc for $C_{191}H_{280}N_{64}O_{53}$ 4320.76, found m/z 4320.5.

Peptide 11. To a solution containng the cyclodecapeptide **8** (5 mg, 3.4 µmol) in 500 µL *t*BuOH/H_2O/AcOH (50:45:5) were added the carbohydrate **10** (3 equiv.). The reaction mixture was stirred for 2 h at room temperature. Then, the pH was adjusted to 8 by addition of a $NaHCO_3$ solution (10%) and the compound **9** *c*[-RGDfK($COCH_2N_3$)-] (6 equiv.) and Cu(0) microsize powder (5 equiv.) were added. The reaction mixture was stirred overnight at room temperature and centrifuged for 5 min. The solution was then purified by RP-HPLC to give the desired compound (8.7 mg, 2 µmol, yield 58 %). Mass spectrum (ES-MS, positive mode) calc for $C_{194}H_{287}N_{65}O_{53}$ 4377.85, found m/z 4377.7.

Peptide 1. The peptide **11** (7.0 mg, 1.59 µmol) was dissolved in 1 mL of anhydrous DMF and the pH adjusted with DIPEA to pH 9. The solution was added to Cy™ 5 Mono NHS Ester (1.2 mg, 1.59 µmol) and stirred for 3 h at room temperature. The product was then purified by RP-HPLC affording the fluorescent peptide **11** as a deep blue solid powder (5.77 mg, 1.14 mmol, yield 72 %). Mass spectrum (ES-MS, positive mode) calc for $C_{227}H_{324}N_{67}O_{60}S_2$ 5015.65, found 5016.7

Peptide 19. The peptide **14** (3.0 mg, 0.73 µmol) was dissolved in 1 mL of anhydrous DMF and the pH adjusted with DIPEA to pH 9. The solution was added to Cy™ 5 Mono NHS Ester (0.54 mg, 0.73 µmol) and stirred for 3 h at room temperature. The product was then purified by RP-HPLC affording the fluorescent peptide **14** as a deep blue solid powder (2.5 mg, 0.53 mmol, yield 73%). Mass spectrum (ES-MS, positive mode) calc for $C_{216}H_{308}N_{65}O_{53}S_2$ 4727.39, found 4727.4.

Peptides 12-18. Peptides **12-16** were prepared as previously described.[14]

Competitive cell adhesion assays. Competitive assay was carried out as described.[13] Briefly, 96-well assay plates were coated for 1 h at room temperature with 5 µg.mL^{-1} vitronectin in PBS and blocked for 30 min with 3 % bovine serum albumin (BSA). Varying amounts of peptides were added simultaneously with 10^5 trypsinated HEK-β3 cells to the wells and the plate was incubated for 30 min at 37 °C. Wells were rinsed three times with cold PBS to remove vitronectin-unbound cells. Attached cells were then fixed with methanol,

stained with methylene blue and quantified. The activity of peptides is expressed as IC50 values (concentration of peptide necessary to inhibit 50% of cell attachment to the vitronectin substrate) and determinates from triplicates in three separate experiments.

Fluorescence Reflectance Imaging (2D-FRI). Female NMRI nude mice (8-10 weeks old, n=6) were injected subcutaneously with human TS/A-pc cells ($1x10^6$ cells per mouse). After tumor growth (~10 days), anesthetized mice were injected intravenously with 10 nmol of Cy5-containing peptide. Mice were illuminated by 633 nm light-emitting diodes equipped with interference filters. Fluorescence images were acquired during 100 ms.

Acknowledgments

This work was supported by the Université Joseph Fourier, the Centre National de la Recherche Scientifique (CNRS), the Institut National de la Santé et de la Recherche Médicale (INSERM), the Institut National du Cancer (INCA), the Nanoscience Foundation and NanoBio (Grenoble).

Notes and references

[a] *Département de Chimie Moléculaire, UMR CNRS/UJF 5250, ICMG FR 2607, 570 rue de la chimie, BP 53, 38041 Grenoble cedex 9, France. Fax: + 33 4 56 52 08 05; Tel: + 33 4 56 52 08 32; E-mail: didier.boturyn@ujf-grenoble.fr*

[b] *Institut Albert Bonniot,INSERM U823,BP 170, 38042 Grenoble cedex 9, France.*

† Electronic Supplementary Information (ESI) available: [details of any supplementary information available should be included here]. See DOI: 10.1039/b000000x/

‡ Footnotes should appear here. These might include comments relevant to but not central to the matter under discussion, limited experimental and spectral data, and crystallographic data.

1 L. A. Thompson and J. A. Ellman, *Chem Rev.*, 1996, **96**, 555.

2 R. C. Ladner, A. K. Sato, J. Gorzelany and M. de Souza, *Drug Discov. Today*, 2004, **9**, 525.

3 H. Kessler, *Angew.Chem. Int. Ed.*, 1982, **21**, 512.

4 a) M. Aumailley, M. Gurrath, G. Müller, J. Calvete, R. Timpl, and H. Kessler, *FEBS Lett.*, 1991, **291**, 50; b) H. M. Ellerby, W. Arap, L. M. Ellerby, R. Kain, R. Andrusiak, G. Del Rio, S. Krajewski, C. R. Lombardo, R. Rao, E. Ruoslahti, D. E. Bredesen and R. Pasqualini, *Nat. Med.*, 1999, **5**, 1032.

5 a) R. O. Hynes, *Nat. Med.*, 2002, **8**, 918; b) K. Temming, R. M. Schiffelers, G. Molema, R. J. Kok, *Drug Resist. Update*, 2005, **8**, 381.

6 M. Mammen, S. K. Choi and G. M. Whitesides, *Angew. Chem., Int. Ed.*, 1998, **37**, 2754.

7 L. L. Kiessling, J. E. Gestwicki and L. E. Strong, *Curr Opin. Chem. Biol.*, 2000, **4**, 696.

8 a) D. Pagé, D. Zanini and R. Roy, *Bioorg. Med. Chem.*, 1996, **4**, 1949; b) U. Sprengard, M. Schudok, G. Kretzschmar, H. Kunz, *Angew. Chem. Int. Ed. Engl.*, 1996, **35**, 321; c) S. M. Dimick, S. C. Powell, A. McMahon, N. Moothoo, J. H. Naismith, and E. J. Toone, *J. Am. Chem. Soc.*, 1999, **121**, 10286; d) P. I. Kitov, J. M. Sadowska, G. Mulvey, G. D. Armstrong, H. Ling, N. S. Pannu, R. J. Read and D. R. Bundle, *Nature*, **403**, 669; e) D. A. Fulton and J. F. Stoddart, *Bioconjugate Chem.*, 2001, **12**, 655; f) J. E. Gestwicki, C. W. Cairo, L. E. Strong, K. A. Oetjen, L. L. Kiessling, , *J. Am. Chem. Soc.*, 2002, **124**, 14922; g) O. Renaudet and P. Dumy, *Org. Lett.*, 2003, **5**, 243; h) D. Arosio, M. Fontanella, L. Baldini, L. Mauri, A. Bernardi, A. Casnati, F. Sansone and R. Ungaro, *J. Am. Chem. Soc.*, 2005, **127**, 3660.

9 a) C.-B. Yim, O. C. Boerman, M. de Visser, M. de Jong, A. C. Dechesne, D. T. S. Rijkers and R. M. J. Liskamp, *Bioconjugate Chem.*, 2009, **20**, 1323; b) N. Trouche, S. Wieckowski, W. Sun, O. Chaloin, J. Hoebeke, S. Fournel and G. Guichard, *J. Am. Chem. Soc.*, 2007, **129**, 13480.

10 a) H. D. Maynard, S. Y. Okada and R. H. Grubbs, *J. Am. Chem. Soc.*, 2001, **123**, 1275; b) R. J. Kok, A. J. Schraa, E. J. Bos, H. E. Moorlag, S. A. Ásgeirsdóttir, M. Everts, D. K. F. Meijer and G. Molema, *Bioconjugate Chem.*, 2002, **13**, 128; c) G. Thumshirn, U. Hersel, S. L. Goodman and H. Kessler, *Chem. Eur. J.*, 2003, **9**, 2717; d) D. Boturyn, J.-L. Coll, E. Garanger, M.-C. Favrot and P. Dumy, *J. Am. Chem. Soc.*, 2004, **126**, 5730; e) X. Montet, M. Funovics, K. Montet-Abou, R. Weissleder and L. Josephson, *J. Med. Chem.*, 2006, **49**, 6087.

11 a) Z. Jin, V. Josserand, J. Razkin, E. Garanger, D. Boturyn, M.-C. Favrot, P. Dumy and J.-L. Coll, *Mol. Imaging*, 2006, **5**, 188; b) J. Razkin, V. Josserand, D. Boturyn, Z. Jin, P. Dumy, M. Favrot, J.-L. Coll and I. Texier, *ChemMedChem*, 2006, **1**, 1069; c) Z. Jin, J. Razkin, V. Josserand, D. Boturyn, A. Grichine, I. Texier, M.-C. Favrot, P. Dumy and J.-L. Coll, *Mol. Imaging*, 2007, **6**, 43; d) L. Sancey, V. Ardisson, L. M. Riou, M. Ahmadi, D. Marti-Batlle, D. Boturyn, P. Dumy, D. Fagret, C. Ghezzi and J.-P. Vuillez, *Eur. J. Nucl. Med. Mol. Imaging*, 2007, **34**, 2037; e) L. Sancey, S. Dufort, V. Josserand, M. Keramidas, C. Rome, A-C. Faure, S. Foillard, S. Roux, D. Boturyn, O. Tillement, A. Koenig, J. Boutet, P. Rizo, P. Dumy and J.-L.Coll. *Int. J. Pharm.*, 2009, **379**, 309; f) J. Dimastromatteo, L. M. Riou, M. Ahmadi, G. Pons, E. Pellegrini, A. Broisat, L. Sancey, T. Gavrilina, D. Boturyn, P. Dumy, D. Fagret and C. Ghezzi. *J. Nucl. Cardiol.*, 2010, DOI: 10.1007/s12350-010-9191-9.

12 a) S. Foillard, Z. Jin, E. Garanger, D. Boturyn, M. Favrot, J.-L. Coll and P. Dumy, *ChemBioChem*, 2008, **9**, 2326; b) S. Foillard, L. Sancey, J.-L. Coll, D. Boturyn and P. Dumy, *Org. Biomol. Chem.*, 2009, **7**, 221.

13 E. Garanger, D. Boturyn, J.-L. Coll, M.-C. Favrot and P. Dumy, *Org. Biomol. Chem.*, 2006, **4**, 1958.

14 M. Galibert, P. Dumy and D. Boturyn, *Angew. Chem. Int. Ed.*, 2009, **48**, 2576.

15 a) K. Rose, *J. Am. Chem. Soc.*, 1994, **116**, 30; b) J. Shao and J. P. Tam, *J. Am. Chem. Soc.*, 1995, **117**, 3893.

16 a) C.W. Tornøe and M. Meldal in Peptides: The Wave of the Future (Eds.: H. Lebl, R. A. Houghten), American Peptide Society, San Diego, 2001, pp. 263; b) C. W. Tørnoe, C. Christensen and M. Meldal, *J. Org. Chem.*, 2002, **67**, 3057; c) V. V. Rostovtsev, L. G. Green, V. V. Fokin, K. B. Sharpless, *Angew. Chem. Int. Ed.*, 2002, **41**, 2596.

17 S. Foillard, M. Ohsten Rasmussen, J. Razkin, D. Boturyn and P. Dumy, *J. Org. Chem.*, 2008**, 73**, 983.

18 B. H. Nicolet and L. A. Shinn, *J. Am. Chem. Soc.*, 1939, **61**, 1615.